Resources and Environment 2022, 12(2): 47-58
DOI: 10.5923/j.re.20221202.02

Proposal of a Systematic Approach for the Identification of Favorable Sites and the Evaluation of the Average Hydroelectric Potential in Ungauged Watersheds with HEC-HMS - Case of the Ramena River (Madagascar)

Justin Ratsaramody

Laboratoire d'Hydraulique, Ecole Supérieure Polytechnique, Université d'Antsiranana, Madagascar

Abstract The identification of favorable sites for hydroelectric development is always a costly and time-consuming operation when it is done starting with field measurements, especially in ungauged watersheds where no measurements (either of discharges or of headwater) are available. Thus, in this work, we propose a systematic approach in 5 steps applicable to any ungauged watershed. It is an approach within the reach of all since both the data (DEM, LULC, soil map, meteorological data) and the tools used are free: QGIS, SAGA for the GIS, R for the calculations and HEC-HMS for the hydrological modeling. To illustrate the method, the case of the Ramena River (Madagascar) is presented with the results obtained at each step. Because of its simplicity of access, the SCS-CN method is proposed in the illustration but it can be replaced by any other equivalent method. An important feature of the study is also the use of a fictitious average year in order to be placed in average conditions and thus reach the objective of evaluating the average hydroelectric potential of a selected site. With the final results being the guaranteed discharges and powers, the proposed approach allows a decision to be made on the development of a site, in isolated or hybrid configuration, and to foresee whether or not additional investigations in the field should be carried out.

Keywords Favorable sites, Fictitious year, Hydrological modeling, HEC-HMS, SCS-CN, Guaranteed discharges

1. Introduction

1.1. Background

With the ever-increasing threat to fossil fuel energy, the use of hydroelectric power can be an interesting alternative, used alone or in a hybrid configuration. Indeed, despite the Sustainable Development Goal (SDG) #7 according to which populations must have access to reliable, sustainable, modern and affordable energy services, the electrification rate in Madagascar is one of the lowest in the world: 26.9% in 2018 for the whole country and only 7.7% in rural areas (https://donnees.banquemondiale.org/indicator/EG.ELC.ACCS.ZS).

Traditionally, the identification of a potential hydroelectric development site is based on the report of local residents following a visual inspection of the presence of a waterfall. Indeed, as these sites are generally far from the usual roads, their access is difficult. If the site is deemed "interesting", field trips are made for topographic and flow measurements that can take years before the data collected is statistically exploitable. Conclusions about the reliability of the site come only after a great deal of time and money has been spent, and in the batch of sites visited and measured, there are many that are rejected because they do not offer the profitability necessary for their operation. This approach is therefore empirical and unreliable.

Before incurring costs for field measurements, it is advisable to know in advance which site will be of interest not only from the point of view of the head H but especially in terms of the flow rate Q, since the power that can be expected from a hydropower site is given by the relationship [1]

$$P = \eta \rho g H Q \quad (1)$$

where P: power [W]; η: general efficiency of the installation [-]; ρ = 1000 kg/m^3 = density of water; g = 9,81 m/s^2 = acceleration of gravity; H = net head [m]; Q = turbine discharge [m^3/s].

The net head H is determined by the topography of the land, by the configuration of the infrastructure and by the equipment making up the development. Even if it can vary

* Corresponding author:
justinratsaramody@yahoo.fr (Justin Ratsaramody)
Received: May 23, 2022; Accepted: Jun. 24, 2022; Published: Jul. 15, 2022
Published online at http://journal.sapub.org/re

according to the water levels upstream and downstream of the power plant, regulation equipment allows to minimize these variations: it can thus be considered as having a fixed value. On the other hand, the flow *Q* is an extremely variable quantity according to time and it is advisable to know this variability to be able to fix the value to be given to *P* because that influences the dimensioning of the equipment of the power station to be projected: number of groups, power of the various groups, types of turbines etc.

As in many countries in the world, almost all watersheds in Madagascar are not gauged, i.e. there are no reliable and/or recent flow measurements. This situation complicates the work of designers in the field of hydroelectric exploitation but also in all fields of exploitation of water resources for agriculture, human consumption etc. The only way to solve this problem is to perform a hydrological modeling which allows to reconstitute the chronicle of these flows according to time by means of tools like HEC-HMS as for example in [2], [3], [4], [5], [6] and [7].

For all these reasons, we propose in this work a systematic approach for the identification of favorable sites on an ungauged watershed and showing the different steps to follow in order to evaluate the powers that can be expected if these sites were to be developed and exploited. This avoids high costs for field trips and allows to have a synthetic view of all possibilities before the field trip.

This systematic approach uses exclusively open source data and tools, which allows anyone to reproduce the methodology without restriction for any river in any ungauged watershed. For illustration in this article, this approach was applied to the case of the Ramena River (Madagascar) which had been considered for a hydroelectric development in the years 2005 but whose site of exploitation had never been definitively fixed.

1.2. Ramena River Location

The Ramena River is a tributary of the Sambirano River and is located in the DIANA Region (Figure 1).

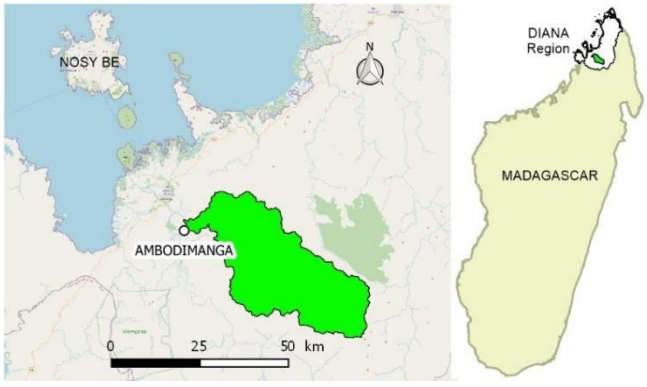

Figure 1. Location of the Ramena River watershed with the village of Ambodimanga as outlet. On the right, location in the island of Madagascar and in the DIANA Region

2. Materials

The materials used are all materials that can be freely acquired on the Internet:

2.1. Data for Watershed Characterization

To characterize the watershed, we used the following data:

- Hypsometry and Hydrography: SRTM Digital Terrain Model with a spatial resolution of 30 m at watershed latitudes (https://earthexplorer.usgs.gov)
- Land use and vegetation cover: Compilation of ESA Sentinel-2 2021 satellite images with a spatial resolution of 10 m [8] available at https://www.arcgis.com/
- Soil: raster file produced by the WRB (*World Reference Base for Soil Resources*) which is the international standard currently used by the IUSS (*International Union of Soil Sciences*) [9] with a spatial resolution of 250 m (HSG: Hydrologic Soil Groups) accessible on https://daac.ornl.gov/

2.2. Meteorological Data

Weather data was obtained in time series format from https://giovanni.gsfc.nasa.gov:

- Daily rainfall data TRMM_3B42_Daily v7 (*Tropical Rainfall Measuring Mission*) covering the period 01/01/1998 to 31/12/2019
- Daily temperature data GLDAS-NOAH (*Global Land Data Assimilation System*) covering the period 01/01/2000 to 31/12/2019

These data are averaged over an area covering a radius of 25 km, applied to the centroid of the Ramena River watershed, thus covering the entire watershed [10], [11], [12].

2.3. Computer Tools

To carry out the calculations of reconstruction of the discharges chronicle at the outlet of the Ramena watershed, we used the following tools:

- GIS processing: free software QGIS (https://www.qgis.org) and SAGA (http://www.saga-gis.org)
- Programming and data processing: open source language R (https://www.r-project.org)
- Hydrological modeling: HEC-HMS v. 4.6.1 (*Hydrologic Engeneering Center - Hydrologic Modeling System*) available at http://www.hec.usace.army.mil/software/hec-hms

3. Methods

The approach proposed in this paper is composed of five essential steps which are, in order:

- Step 1: Identification of favorable sites
- Step 2: Characterization of the total river catchment
- Step 3: Processing of rainfall data
- Step 4: Hydrological modeling of the watershed drained by each of the sites identified in Step 1
- Step 5: Exploitation of the results obtained

3.1. Step 1: Identification of Favorable Sites

According to equation (1), the hydroelectric power obtained at a site depends on both the net head H and the discharge Q, in other words, on the topography of the land at the site and the surface drained by the watershed of which the site is the outlet. Theoretically, any site on the river could be suitable. However, for economic reasons, it is more advantageous to choose a site where the local slope is high. The higher the slope, the shorter the length of the penstock required to bring the water from the dam to the powerhouse (and therefore the lower the capital cost).

Therefore, the identification of favorable sites is conducted by tracing the longitudinal profile of the river and then setting a criterion on the surface drained (> 150 km2 in our case), a criterion on the local slope (> 10% in our case) and a third criterion on the abundance of flows (presence of a major tributary upstream of the site). This longitudinal profile was drawn with QGIS from the Digital Terrain Model.

3.2. Step 2: Characterization of the Total River Watershed

In this step, the entire river watershed must be considered, i.e., the outlet must be chosen so that the upstream portion of this outlet includes all the potential sites determined in Step 1. This step consists of classical GIS processing (with QGIS and SAGA) and the expected results are:

- hypsometric characteristics and the hydrographic network
- soil characteristics
- Land use and land cover map (LULC)
- Curve Number (CN) runoff coefficient spatial distribution map

The objects manipulated in this step are originally rasters, but they can be easily converted to vector objects to determine their quantitative properties.

The map of the spatial distribution of the CN runoff coefficient was obtained by combining the soil map and the LULC map. However, all these rasters had to be resampled beforehand in order to obtain the same spatial resolution based on the most accurate raster; in our case, this spatial resolution was 10 m (LULC raster).

3.3. Step 3: Processing of Rainfall Data

Even if we have a time series of rainfall data (daily rainfall from 01/01/1998 to 31/12/2019 in our case), the evaluation of the average hydroelectric potential requires that these rainfall data are also brought back to a year with average weather conditions. This average year will then be a fictitious year (say 2035) established as follows:

- The fictitious month of January 2035 will be the average January from 1998 to 2019
- The fictitious month of February 2035 will be the average month of February from 1998 to 2019
- And so on

This gives the daily rainfall data for the fictitious year 2035.

3.4. Step 4: Hydrological Modeling

Since the watershed is not gauged, hydrological modeling is required. For each of the identified sites, the objective of the hydrological modeling is to determine the discharge at the outlet by reconstructing the physical processes that occur in the watershed (Figure 2):

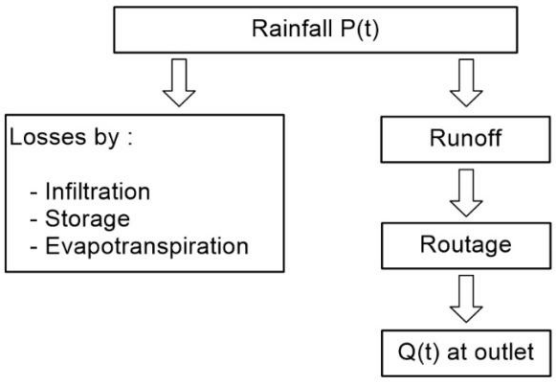

Figure 2. Hydrologic processes for reconstructing outflow at each site

3.4.1. Assessment of Infiltration and Storage Losses

For this systematic approach, the recommended method for evaluating losses is the NRCS (*Natural Resources Conservation Service*) Curve Number (CN) method. This is a method that includes infiltration losses and storage losses but not evapotranspiration losses: it is therefore necessary to evaluate these evapotranspiration losses in another way.

3.4.2. Assessment of evapotranspiration losses

For the evaluation of evapotranspiration losses, the method of Hamon [13] [14] can be used, which requires only easily accessible data. According to this method:

$$ETP = \frac{29.8 N e_s(T)}{2T + 273}$$

$$\text{where} \quad e_s(T) = 0.6108 \exp\left[\frac{17.27T}{T + 237.3}\right] \tag{2}$$

ETP: potential evapotranspiration (mm); e_s: saturation vapour pressure (Pa); *T*: mean temperature (℃); *N*: number of hours of sunshine given by

$$N = 2 \arccos\left[-\tan\varphi \tan\delta\right] \frac{12}{\pi}$$

$$\text{where} \quad \delta = 1 + 0.033 \cos\left(\frac{2\pi}{365} J\right) \tag{3}$$

where φ: latitude; δ: declination and *J*: Julian day

The ETP assumes that the amount of water available for this evapotranspiration is unlimited. The actual evapotranspiration (ETR) is then calculated as follows:

$$\begin{cases} ETR = ETP & \text{if } P > ETP \\ ETR = 0 & \text{if } P \le ETP \end{cases} \quad (4)$$

where *P* (mm): average daily rainfall. The calculation time step is therefore the day for the different equations (2) to (4).

3.4.3. Base Flow

Base flow can be ignored if no such data is available, which is the most common case in ungauged watersheds. This would simply means that the simulated flows obtained by the hydrological modeling will actually be lower than the actual flows in the field.

In our case, we had as data the specific flow q_s (m3/s/km2) of the whole Ramena river catchment [15] and which corresponded to the absolute minimum daily flow (the most pessimistic value). The base flow can then be obtained by multiplying this specific flow by the area of the watershed.

3.4.4. Rainfall-Runoff Transformation Method

The recommended method is the SCS-CN (Soil Conservation Service - Curve Number) runoff model associated with the SCS unit hydrograph. It is an empirical method but is among the most widely used methods in the world because of its high agreement between theoretical results and observed values. In this method, the hydrological impact of land use, vegetation cover and infiltration capacity is taken into account by a single parameter which is the CN (Curve Number). The SCS-CN model is based on the water balance equation [16]:

$$P = I_a + F + R \quad (5)$$

P: rainfall (mm); I_a : initial abstraction (mm); *F*: cumulative infiltration (mm) which does not include I_a and *R* is direct runoff (mm).

It is furthermore assumed that there is a direct relationship between the initial abstraction and the maximum potential abstraction, *S*, according to [16] [17].

$$\frac{R}{P - I_a} = \frac{F}{S} \text{ and } I_a = \lambda S \quad (6)$$

S: maximum retention potential (mm) after the onset of runoff and λ is a regional parameter depending on geographical and climatic factors [16]. In its original form [19], the regional parameter is λ=0.2 which leads to the fundamental equation of the SCS-CN model:

$$\begin{cases} R = \dfrac{(P - 0.2S)^2}{P + 0.8S} & \text{if } P > 0.2S \\ R = 0 & \text{if } P \le 0.2S \end{cases} \quad (7)$$

To calculate *S*, the empirical relationship between *S* and *CN* is [5], [17]:

$$S = \frac{25400}{CN} - 254 \quad (8)$$

As the excess rain does not instantaneously transform into runoff, the latter occurs only after a lag time which, for ungauged catchments, is estimated by the SCS by [18]:

$$T_{lag} = 0.6T_c \quad (9)$$

where T_c is the time of concentration, which is evaluated according to the Passini relationship (valid for rural watersheds larger than 4000 ha):

$$T_c = 1.44 \frac{(AL)^{1/3}}{\sqrt{S}} \quad (10)$$

where *A*: watershed area [ha]; *L:* length of longest water path [m]; *S*: slope [%]; T_c : Time of concentration [min].

For normal (moisture) conditions, CN, denoted CN_{II} , is given by equation (8). For different antecedent conditions prior to the date of calculations, we have the following relationships [19]:

$$CN_I = \frac{4.2CN_{II}}{10 - 0.058CN_{II}}; CN_{III} = \frac{23CN_{II}}{10 - 0.12CN_{II}} \quad (11)$$

CN_I : for dry antecedent conditions and CN_{III} , for wet antecedent conditions. Generally, these conditions are for 5 days before the current day.

3.4.5. Hydrograph Routing Modeling

The division into sub-watersheds is necessary to take into account the particularities between the different zones in the watershed of which the selected site is the outlet. This increases the accuracy of the results, particularly because of the diversity of the characteristics of these different areas: relief, flow paths, soil types, land use, soil cover, etc. After applying the loss assessment methods and the SCS-CN rainfall-runoff transformation model described above, the resulting hydrographs must be routed along the stream reaches to the outfall, i.e. the selected site.

For this, the Muskingum method was used. This method is presented in the form of two equations which are the continuity equation and the storage equation at a time *t* [20]:

$$\frac{dS_t}{dt} = I_t - O_t \quad (12)$$

$$S_t = K\left[XI_t + (1 - X)O_t\right] \quad (13)$$

Equations (12) and (13) depend only on the parameters K and X which can be taken equal to mean values of 0.5 and 0.25, respectively.

3.5. Step 5: Exploitation of the Results Obtained

For each site, the results of the previous hydrological modeling lead to flow versus time records for the fictitious

year. For different heads *H*, the expected power is then given by equation (1). These results can be processed in several ways, but the most important ones are given below.

3.5.1. Empirical Probabilities

Plotting position: by ranking the series of daily flows obtained in descending order, we can determine the empirical probabilities using, for example, the Weibull relation:

$$p_0 = \Pr(Q \le Q_0) = \frac{r}{N+1} \tag{14}$$

p_0: probability of occurrence of the flow Q_0; *r*: rank of the value Q_0 in the series ranked in descending order; *N*: total number of values in the series (i.e. *N* = 365 for the fictive year 2035)

Equation (14) thus provides the probability of occurrence of a certain flow Q_0 in terms of fraction of the year. In general, the scatter plot obtained can be approximated by an empirical relationship of the form:

$$Q = a\exp(bp) \tag{15}$$

where *Q* is the flow rate corresponding to probability *p*; *a* and *b* are fitting coefficients.

3.5.2. Classified and Guaranteed Flows - Guaranteed Powers

For example, for a hybrid power plant, one often needs to know for how many months one can use the power supplied by the hydroelectric plant corresponding to a given site. For this purpose, the classical way of using the classified and guaranteed flows is to replace the probability *p* in the adjusted expression (15) with the following values:

$$p = \frac{m}{12}; m = 1, 2, \ldots, 12 \tag{16}$$

For each site, this will give the values of the guaranteed flows m months out of 12: $Q_1, Q_2, \ldots, Q_{12}$.

Using equation (1), these flow values can be converted into power values according to the exploitable heads at each site. As for the energy produced, it can be evaluated as follows:

$$E = P_m \Delta t_m \tag{17}$$

where P_m is the guaranteed power for *m* months and Δt_m is the number of hours contained in the *m* months i.e.:

$$\Delta t_m \approx m \times 30 \text{ days} \times 24 \text{ hr} \tag{18}$$

4. Results for Ramena River

The method described above was applied to the Ramena River watershed (Figure 1) with the following step-by-step results.

4.1. Results of the Identification of Favorable Sites

Using the method described, three sites were identified based on the following criteria:

1. Slope of the watercourse at the site > 10%.
2. Watershed area drained by the site > 150 km2.
3. The site is located downstream of a major tributary to benefit from additional flow inputs.

By staying only on the criteria of slope, it had led to a very high number of favorable sites (148 in our case). By adding the second and third criteria above, a more reduced selection of sites could be made. We can thus see in Figure 3 that, compared to Site A, Site B benefits from the contribution of two important tributaries (Morafeno River on the right bank and Ampanasy River on the left bank). The same is true of Site C, where the inflow from the Androatra tributary is added to all the inflows from the rivers upstream.

Table 1. Characteristics of the sites identified for the Ramena River watershed

Site	Area [km2]	Perimeter [km]	River Length [km]	Outlet Elevation [m]	Slope
A	391.3	122.4	38.2	414	25.5%
B	742.0	186.5	55.0	200	13.2%
C	953.7	226.3	226.3	51	19.8%

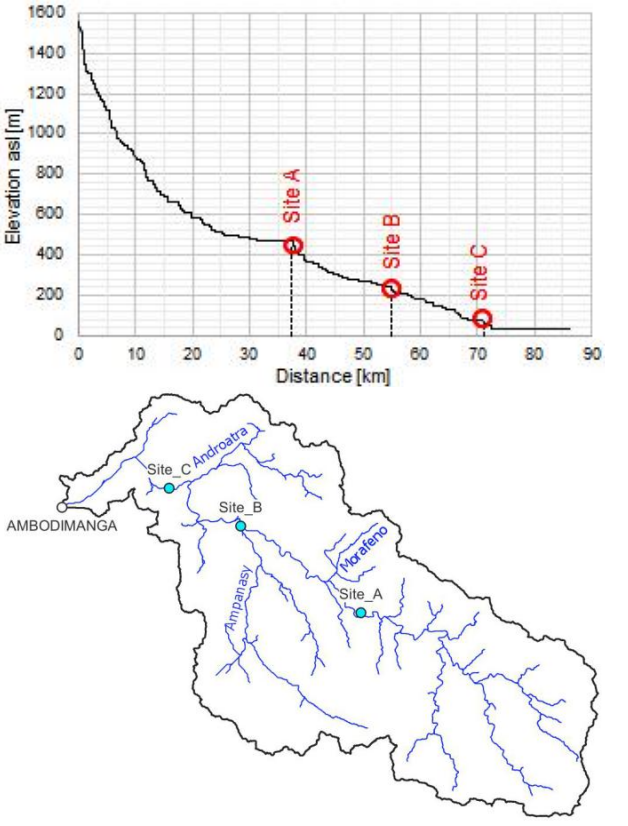

Figure 3. Location of favorable sites. Left: Longitudinal profile of the main river. Right: Location of sites in the Ramena River watershed

4.2. Total Watershed Characterization Results

Hypsometric and hydrographic characteristics:

Figure 4.

Total length of the main Ramena river from its source to the Ambodimanga outlet: L = 86.2 km.

HSG and LULC:

Figure 5.

Gridded CN values:

Figure 6.

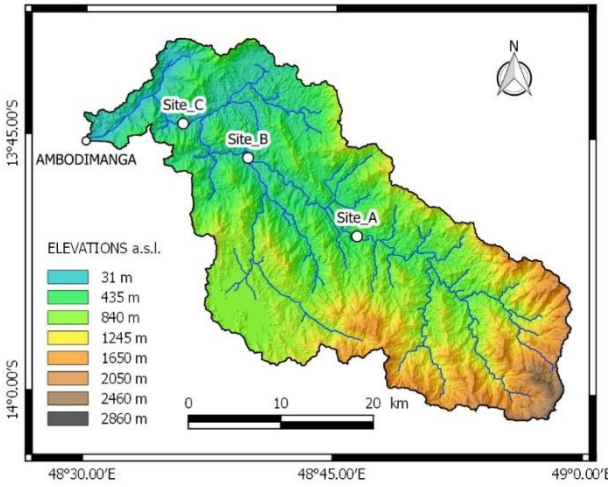

Figure 4. Ramena River Watershed (area A = 1030 km2, perimeter P = 261 km)

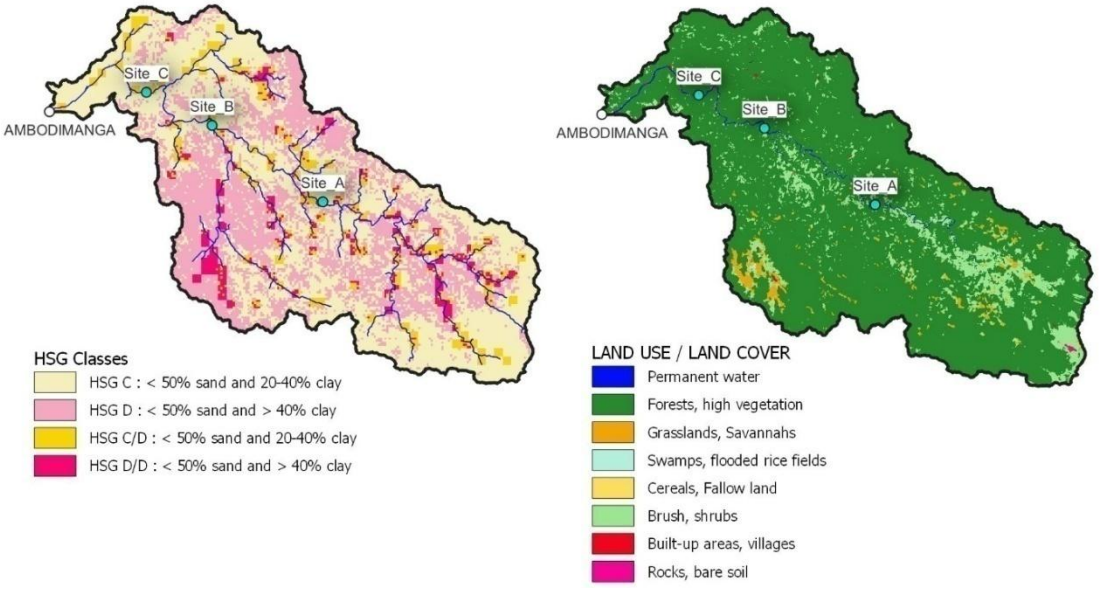

Figure 5. Left: HSG Classes (C: moderately high runoff potentiel, D: high runoff potentiel, C/D et D/D: high runoff potentiel unless drained). Right: Land Use / Land Cover

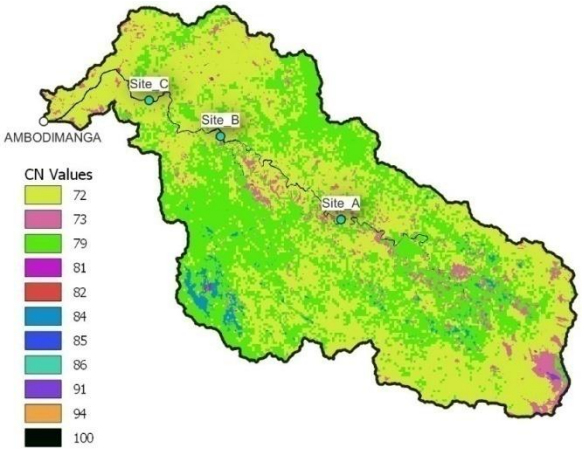

Figure 6. Gridded CN values (random colors)

4.3. Results of Meteorological Data Processing

By applying the described method, the results obtained for the Ramena River are in Table 2.

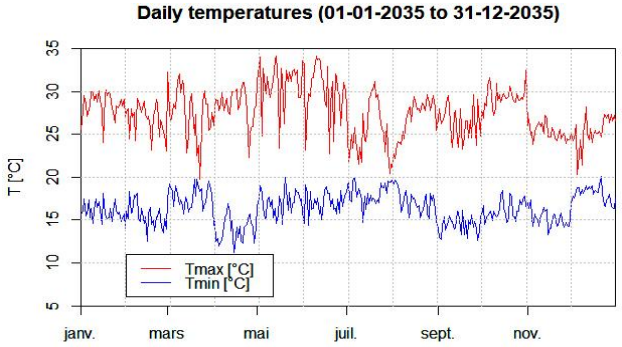

Figure 7. Daily minimum and maximum temperatures for the fictitious mean year 2035

The evaluation of evapotranspiration according to equations (2) to (4) required daily minimum and maximum temperature data which are shown in Figure 7.

After calculating evapotranspiration, the daily rainfall distribution for the fictitious year 2035 had given Figure 8.

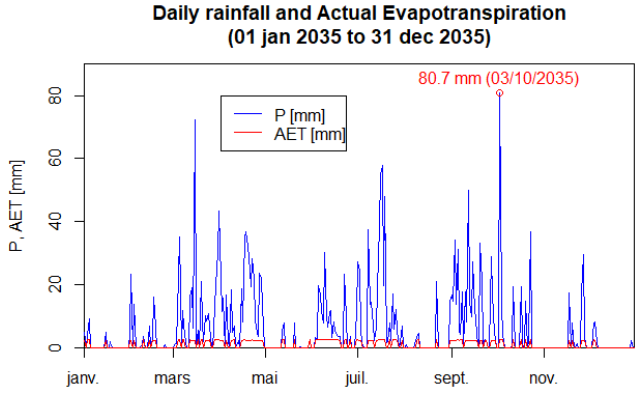

Figure 8. Daily rainfall and real evapotranspiration for the fictitious average year 2035

4.4. Hydrological Modeling Results

Division into sub-watersheds

For each of the 3 sites, the division into sub-watersheds was done automatically by the HEC-HMS software.

Number of sub-watersheds:

- Site A: 05
- Site B: 13
- Site C: 15

The number of subwatersheds per site could have been reduced by merging some of them, but the more subwatersheds, the greater the accuracy.

Results of the rainfall-flow transformation

For the Ramena River case and for the fictitious year 2035, these results are shown in Figure 12.

Figure 12 shows that the flow chronicles have the same shapes, which is normal because we have the same rainfall input data. The difference is in the values of the flows which depend on the characteristics of the drained surfaces which are different according to the sites.

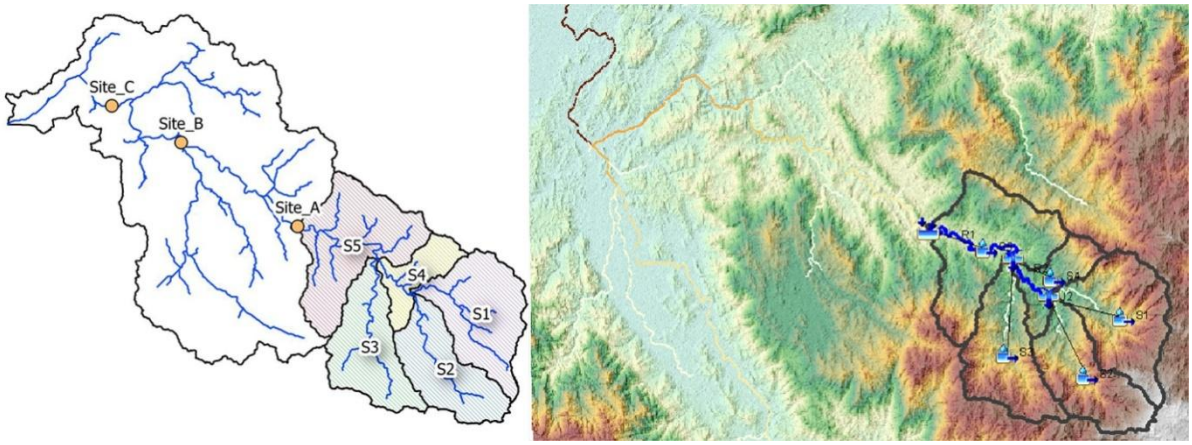

Figure 9. Watershed of Site A divided into sub-watersheds. Left: representation in QGIS. Right: stylized representation on a terrain background in HEC-HMS

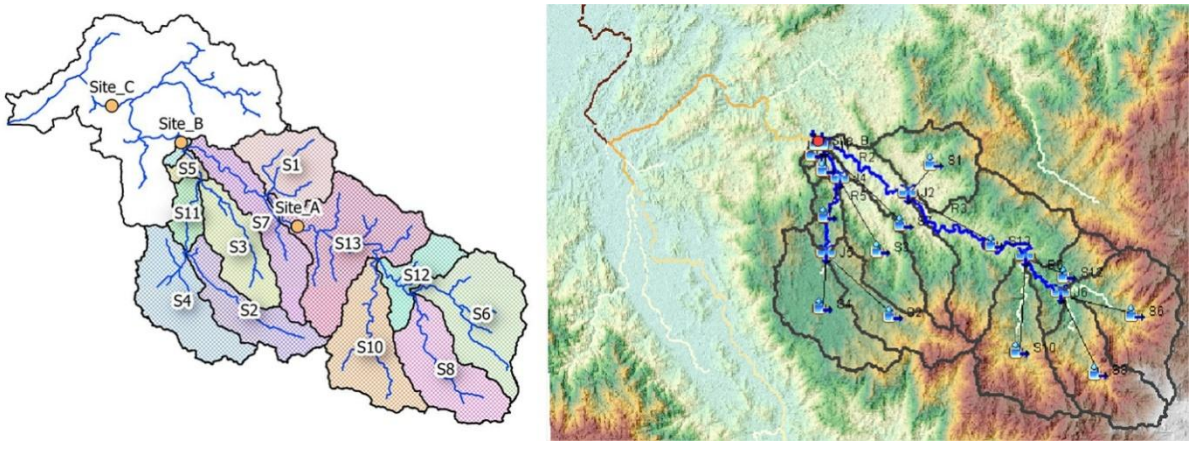

Figure 10. Watershed of Site B divided into sub-watersheds. Left: representation in QGIS. Right: stylized representation on a terrain background in HEC-HMS

Table 2. Composition of the fictitious year 2035

Fictitious month	Real year	P [mm/month]	Fictitious month	Real year	P [mm/month]
January	2008	448.0	**July**	2019	19.8
February	2005	372.9	**August**	2008	31.6
March	2011	418.3	**September**	1998	25.1
April	2006	195.0	**October**	2012	76.5
May	2000	79.8	**November**	2011	192.3
June	2005	22.9	**December**	2000	404.5
				TOTAL =	**2286.8**

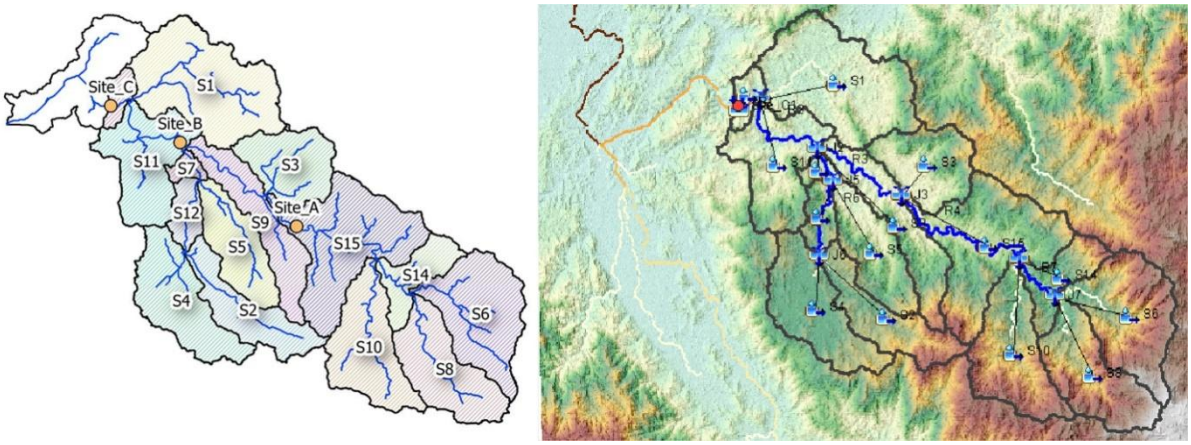

Figure 11. Watershed of Site C divided into sub-watersheds. Left: representation in QGIS. Right: stylized representation on a terrain background in HEC-HMS

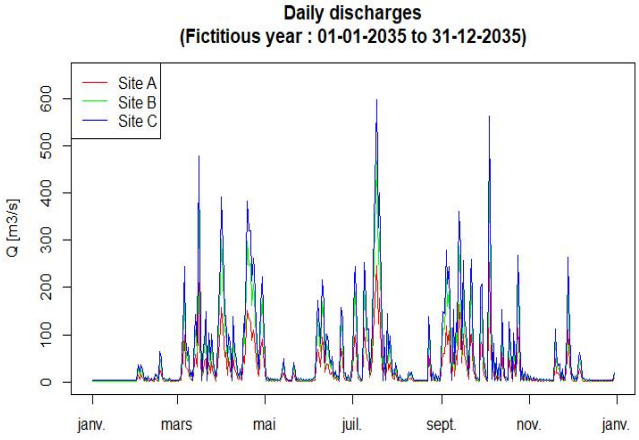

Figure 12. Daily flows for the 3 sites in the fictitious year 2035

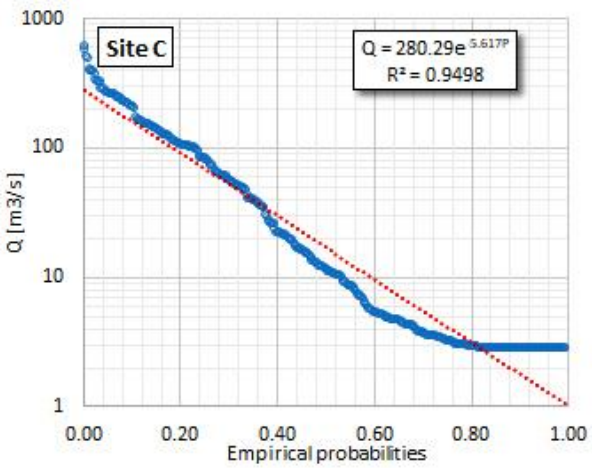

Figure 13. Site C: simulated flows vs. empirical probabilities fitted by an exponential function

4.5. Results of the Exploitation of the Results Obtained

4.5.1. Empirical Probabilities

By application of equation (15), the different values of the simulated flows as a function of the empirical probabilities had been fitted with an exponential curve as, for example, in Figure 13 for Site C.

For the three Ramena River sites, the adjustment coefficients are summarized in Table 3. For each of the sites, the coefficient of determination R2 is close to 0.95, which shows an excellent fit.

Table 3. Fitting coefficients of equation (15) for the Ramena River

	Site A	Site B	Site C
a	0.2046	0.3624	0.5042
b	4×10^{-15}	8×10^{-15}	4×10^{-14}

Subsequently and using the previous fitting curves, it is possible to evaluate the potential powers as a function of the net height which had given Figure 14.

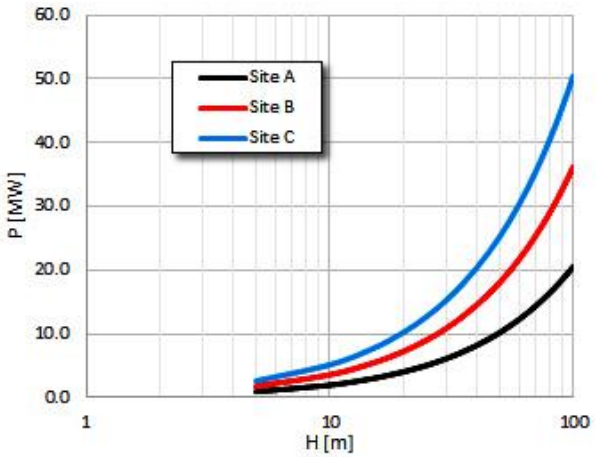

Figure 14. Potential power P versus head H for the Ramena River

4.5.2. Classified and Guaranteed Flows - Guaranteed Powers

Table 4. Classified and guaranteed flows for 1 year for the Ramena River

Guaranted number of months	Q Site A [m3/s]	Q Site B [m3/s]	Q Site C [m3/s]
1	70.8	137.2	175.5
2	44.4	85.9	109.9
3	27.9	53.7	68.8
4	17.5	33.6	43.1
5	11.0	21.1	27.0
6	6.9	13.2	16.9
7	4.3	8.2	10.6
8	2.7	5.2	6.6
9	1.7	3.2	4.1
10	1.1	2.0	2.6
11	0.7	1.3	1.6
12	0.4	0.8	1.0

Although the curves in Figure 14 show the power that can potentially be obtained for different heads at each site, they do not provide any information on how long that power can be obtained. By applying equations (16) through (18), it is possible to determine the classified and guaranteed flows and the guaranteed powers, both as a function of time. For the illustrative case of the Ramena River, this had given Table 4.

Graphically, this resulted in Figure 15:

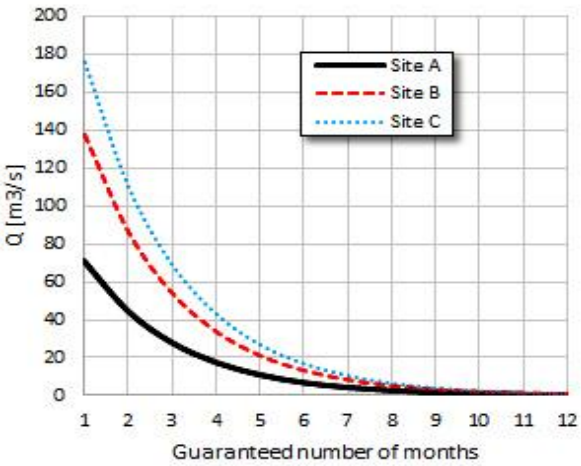

Figure 15. Classified and guaranteed flows for the Ramena River

It is therefore possible to determine the guaranteed powers as a function of the head H for a given number of months during 1 year (Figure 16).

Of course, as the number of months increases, the guaranteed power decreases. For example, in Figure 16, the same 20 m head would give a power of 2.9 MW, 5.6 MW and 7.2 MW for sites A, B and C, respectively, for a duration of 4 months while, for a duration of 8 months, it would give a power of 1.1 MW, 2.2 MW and 2.8 MW, again for the 3 sites A, B and C, respectively.

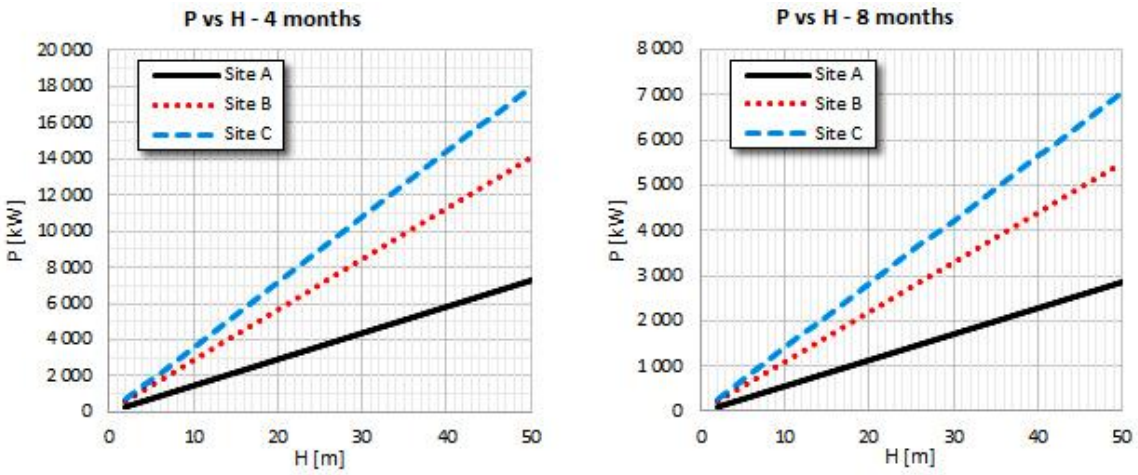

Figure 16. Examples of guaranteed power curves as a function of head (left: 4 months; right: 8 months) for the 3 Ramena River sites

5. Discussion of Methods and Results

5.1. On Step 1: Identification of Favorable Sites

The use of GIS to carry out this identification had already been used by other researchers (e.g. [21], [22], [1] etc.), the fundamental difference with the present study is the addition of two other criteria, i.e. the surface drained (A > 150 km2) and the presence of a major tributary upstream of the site's outlet. Indeed, with only the criterion of slope (>10%), we had found 148 sites in the case of the Ramena River, which would have been impossible to analyze one by one. In our case, we were finally able to identify the three sites named: Site A, Site B and Site C.

Very recent studies in the Philippines [26] have emphasized the importance of the spatial resolution of the DEM used, 5 m in their case, in the accuracy of the river profile. In the present study, for reasons of method reproducibility, a less spatially accurate DEM (30 m) was used, but it is much more readily available (https://earthexplorer.usgs.gov).

5.2. On Step 2: Characterization of the Total Watershed of the River

In the hydrological model used, it was assumed that land use and land cover remained unchanged throughout the simulation (fictitious year 2035), which is not entirely true in reality [7]. This assumption had necessarily influenced the runoff results and, ultimately, the flows obtained at each site. It is possible to improve this assumption by considering month-specific LULCs from satellite image data processed by classification and averaged over the month of interest. However, this work was not necessary here since the objective was only to roughly evaluate the potential at each site before going to the field and then making the necessary measurements.

5.3. On Step 3: Processing of Rainfall Data

The choice of using a fictitious year instead of a real year was justified by the fact that average weather conditions were to be used. It should be noted that this was based on the average months of all the observation data, which made it possible to keep the daily data corresponding to these average months. In addition, the consideration of evapotranspiration was absolutely necessary because it can be high in the Ramena River watershed [15], but this depends on the characteristics of the region under study.

5.4. On Step 4: Hydrological Modeling

The methods we used in the hydrological modeling mainly based on the Curve Number (CN) are methods that have already been used by many studies around the world for several decades and implemented with HEC-HMS that had given acceptable results when compared to the values measured in the field. Indeed, the choice of HEC-HMS software is largely justified by its ability to model and reproduce the model and sub-models used in this study, namely a physically based conceptual model. It has also been successfully used and continues to be used for ungauged watersheds for decades by various researchers such as [2] in India, [23] in Indiana (USA), [3] in Morocco, [4] in India, [6] in Malaysia, [24] in Central Europe etc. as well as some of the researchers already mentioned above.

On the question of base flow, we were fortunate to have the specific flow for the Ramena River watershed. However, even without such data, this is not a problem and can even be considered beneficial in a certain sense because it means that the flows found in the simulated hydrograph are actually lower than the actual flows, especially during the dry season.

5.5. On Step 5: Exploitation of the Results Obtained

The form of the results (classified and guaranteed flows, guaranteed powers) presented in this study is the one that assumes the use of a hybrid power plant, i.e. when another form of additional energy (thermal, photovoltaic, etc.) must be present to compensate for the insufficiencies of the purely hydroelectric energy.

Some authors prefer the notion of dependable flow which is none other than the flow with a guarantee higher than 80% or 90% [1] [25] to evaluate the hydroelectric potential of a site from the FDC (Flow Duration Curve) as in Figure 13. Here, this can be done easily from equation (14) or fitting equations (15) with the parameters in Table 3 to calculate the empirical probabilities and retain only the probabilities greater than 0.8. In the case of the Ramena River, this resulted in the following Table 5:

Table 5. Dependable flows in m3/s at the 3 sites of the Ramena River according to the fitting equations

Proba	Site A	Site B	Site C
0.80	1.28	2.44	3.13
0.85	0.97	1.84	2.37
0.90	0.73	1.39	1.79
0.95	0.55	1.05	1.35

The concept of dependable flow is especially useful when it is envisaged to operate the hydroelectric plant continuously practically throughout the year without the contribution of any other energy source as in a hybrid plant.

6. Conclusions

In this work, a systematic method was proposed that describes in detail how to identify sites suitable for hydroelectric development, how to evaluate the potential of each selected site and how to exploit the results obtained. In order to make it accessible to anyone and anywhere, open source data and tools were used. To illustrate this method and to describe the results to be obtained at each step, the example of the Ramena River (Madagascar), whose watershed is completely ungauged (total absence of flow measurements) was given.

Despite the inaccuracies inherent to the fact that the basin

is ungauged (routing parameters etc.), we believe that the method is sufficiently accurate to identify where to focus efforts and then conduct the necessary field measurements (topographic measurements to determine the head, flow measurements etc.). Once the measurements are made, these inaccuracies will be removed by calibrating the theoretical model. The method also makes it possible to foresee which type of development is possible: indeed, the flows and the guaranteed powers will allow the dimensioning of a hybrid development.

Furthermore, once one or more sites are identified, the next step would be to apply weighted economic and environmental criteria to assess the actual suitability of the site [27], particularly with respect to the electrical transmission system. Furthermore, when several sites are eligible on the same river, further environmental studies are needed as recent studies [28] have shown the influence of spatial density of small hydro facilities (< 10 MW) and environmental flow on hydro potential.

For the present study, the objective of the method was to help the decision-makers on the purely technical part of the water resource, but it is obvious that other criteria, such as those indicated above, can intervene in the final choice: presence or necessity of creation of access roads, length of the electric transport and distribution network, etc.

REFERENCES

[1] E. Hidayah, Indarto, S. Wahyuni (2017). Proposed method to determine location of hydropower plant: application at Rawatamtu watershed, East Java. *Procedia Engineering* 171 (2017) 1495 – 1504. DOI: https://doi.org/10.1016/j.proeng.2017.01.480.

[2] Meenu R., S. Rehana, P.P. Mujumdar (2013). Assessment of hydrologic impacts of climate change in Tunga–Bhadra river basin, India with HEC-HMS and SDSM. *Hydrological Processes* 27, pp 1572–1589 (2013). https://doi.org/10.1002/hyp.9220.

[3] Ahbari A., L. Stour, A. Agoumi, N. Serhir (2018). Estimation of initial values of the HMS model parameters: application to the basin of Bin El Ouidane (Azilal, Morocco). *Journal of Materials and Environmental Sciences*, 2018, 9 (1), pp. 305-317. https://doi.org/10.26872/jmes.2018.9.1.34.

[4] Koneti S., S.L. Sunkara, P.S. Roy (2018). Hydrological Modeling with Respect to Impact of Land-Use and Land-Cover Change on the Runoff Dynamics in Godavari River Basin Using the HEC-HMS Model. *ISPRS International Journal of Geo-Information*, 2018, 7, 206; https://doi.org/10.3390/ijgi7060206.

[5] Ouédraogo W.A.A., J.M. Raude, J.M. Gathenya (2018). Continuous Modeling of the Mkurumudzi River Catchment in Kenya Using the HEC-HMS Conceptual Model: Calibration, Validation, Model Performance, Evaluation and Sensitivity Analysis. *Hydrology* 2018, 5, 44; https://doi.org/10.3390/hydrology5030044.

[6] Adilah N., S. Nuramirah (2019). Estimating flow rate in gauged and ungauged stations in Kuantan river basin using Clark method in HEC-HMS. *IOP Conferences Series: Earth and Environmental Science*, 244 (2019) 012014, https://doi.org/10.1088/1755-1315/244/1/012014.

[7] Paudel R.C., K. Basnet and B. Sherchan (2019). Application of HEC-HMS Model for Runoff Simulation: A Case Study of Marshyangdi River Basin in Nepal. *Proceedings of IOE Graduate Conference*, 2019-Winter, Vol. 7, December, ISSN: 2350-8914 (Online).

[8] Karra K., C. Kontgis, Z. Statman-Weil, J. Mazzariello., M. Mathis, S. Brumby (2021). Global land use/land cover with Sentinel-2 and deep learning. *International Geoscience and Remote Sensing Symposium* (IGARSS), IEEE, 2021.

[9] Ross C.W., L. Prihodko, S. Kumar, W. JI, N.P. Hanan (2018). *Global Hydrologic Soil Groups (HYSOGs250m) for Curve Number-Based Runoff Modeling*, Oak Ridge, Tennessee, USA, https://doi.org/10.3334/ORNLDAAC/1566.

[10] Goddard Earth Sciences Data and Information Services Center (2016), TRMM (TMPA-RT) Near Real-Time Precipitation L3 1 day 0.25 degree × 0.25 degree V7, Edited by Andrey Savtchenko, Greenbelt, MD, *Goddard Earth Sciences Data and Information Services Center* (GES DISC), Accessed: 2021-09-12, https://doi.org/10.5067/TRMM/TMPA/DAY-E/7.

[11] Beaudoing H., M. Rodell, NASA/GSFC/HSL (2020), GLDAS Noah Land Surface Model L4 monthly 1.0 × 1.0 degree V2.1, Greenbelt, Maryland, USA, *Goddard Earth Sciences Data and Information Services Center* (GES DISC), Accessed: 2021-09-12, https://doi.org/10.5067/LWTYSMP3VM5Z.

[12] Rodell M., P.R. Houser, U. Jambor, J. Gottschalck, K. Mitchell, C. Meng, K. Arsenault, B. Cosgrove, J. Radakovich, M. Bosilovich, J.K. Entin, J.P. Walker, D. Lohmann, D. Toll (2004). The Global Land Data Assimilation System, *Bulletin of American Meteorologic Society*, 85, pp. 381-394, https://doi.org/10.1175/BAMS-85-3-381.

[13] Guo D., S. Westra, H.R. Maier (2016). An R package for modelling actual, potential and reference evapotranspiration. *Environmental Modelling & Software*. Volume 78, April 2016, Pages 216-224. DOI: https://doi.org/10.1016/j.envsoft.2015.12.019.

[14] Lang D., J. Zheng, J. Shi, F. Liao, X. Ma, W. Wang, X. Chen, M. Zhang (2017). A Comparative Study of Potential Evapotranspiration Estimation by Eight Methods with FAO Penman–Monteith Method in Southwestern China. *Water* 2017, 9, 734. https://dx.doi.org/10.3390/w9100734.

[15] P. Chaperon, J. Danloux, L. Ferry (1993). *Fleuves et Rivières de Madagascar*. Ed. ORSTOM, Paris (France), 883 p.

[16] Wang D., L. Qin, B. Chang, M. Wang, W. Zhang (2015). "Application of SCS-CN Model in Runoff Estimation", ISM3E: *International Symposium on Material, Energy and Environment Engineering*. https://doi.org/10.2991/ism3e-15.2015.14.

[17] Santikari V.P., L.C. Murdoch (2018). Including effects of watershed heterogeneity in the curve number method using variable initial abstraction. *Hydrology and Earth System Sciences*, 22, pp. 4725–4743, 2018. https://doi.org/10.5194/hess-22-4725-2018.

[18] USACE (2000). "Hydrologic Modeling System HEC-HMS:

Technical Reference Manual", Hydrologic Engineering Center (2000). https://www.hec.usace.army.mil/software/hec-hms/documenttion/HEC-HMS_Technical%20Reference%20Manual_(CPD-74B).pdf.

[19] USDA (1986). *Urban Hydrology for Small Watershed, Technical Release TR-55*. 210-VI-TR-55, Second Ed. (June 1986). https://www.nrcs.usda.gov/Internet/FSE_DOCUMENTS/stelprdb1044171.pdf.

[20] Ehteram M., F.B. Othman, Z.M. Yaseen, H.A. Afan, M.F. Allawi, M.B.A. Malek, A.N. Ahmed, S. Shahid, V.P. Singh, A. El-Shafie (2018). "Improving the Muskingum Flood Routing Method Using a Hybrid of Particle Swarm Optimization and Bat Algorithm", *Water*, vol. 10 (807), pp.1-21, https://doi.org/10.3390/w10060807.

[21] Bergstrom D., C. Malmros (2005). Finding Potential Sites for Small-Scale Hydro Power in Uganda: A Step to Assist the Rural Electrification by the Use of GIS, *Seminar series nr 121, Geobiosphere Science Centre Physical Geography and Ecosystems Analysis Lund University* Sölvegatan 12 S-223 62 Lund Sweden.

[22] Setiawan D. (2015). Potential Sites Screening for Mini Hydro Power Plant Development in Kapuas Hulu, West Kalimantan: a GIS approach, *Energy Procedia* 65 (2015) 76– 82. DOI: https://doi.org/10.1016/j.egypro.2015.01.034.

[23] Jeon J.H., K.J. Lim, B.A. Engel (2014). Regional Calibration of SCS-CN L-THIA Model: Application for Ungauged Basins. *Water* 2014, 6, pp 1339-1359; https://doi.org/10.3390/w6051339.

[24] Caletka M., M.S. Michalková, P. Karásek, P. Fucík (2020). Improvement of SCS-CN Initial Abstraction Coefficient in the Czech Republic: A Study of Five Catchments. *Water* 2020, 12, 1964; https://doi.org/10.3390/w12071964.

[25] Salim S., M. Poling (2021). River Flow Modelling for Sustainable Operation of Hydroelectric Power Plant in the Taludaa-Gorontalo Watershed. *Indonesian Journal of Geography* Vol.53, No. 3, 2021 (400-407). DOI: http://dx.doi.org/10.22146/ijg.64627.

[26] Torrefranca I., Otadoy R.E., Tongco A. (2022). Incorporating Landscape Dynamics in Small-Scale Hydropower Site Location Using a GIS and Spatial Analysis Tool: The Case of Bohol, Central Philippines. *Energies* 2022, 15, 1130. https://doi.org/10.3390/en15031130.

[27] Atwongyeire J.R., Palamanit A., Bennui A., Shakeri A., Techato K., Ali S. (2022). Assessment of Suitable Areas for Smart Grid of Power Generated fromRenewable Energy Resources in Western Uganda. *Energies* 2022, 15, 1595. https://doi.org/10.3390/en15041595.

[28] Quaranta E., Bódis K., Kasiulis E., McNabola A., Pistocchi A. (2022). Is There a Residual and Hidden Potential for Small and Micro Hydropower in Europe? A Screening-Level Regional Assessment. *Water Resources Management* (2022) 36:1745–1762. https://doi.org/10.1007/s11269-022-03084-6.